Available online at www.sciencedirect.com
ScienceDirect
Journal of the European Ceramic Society 28 (2008) 2389–2397
www.elsevier.com/locate/jeurceramsoc

Phase diagram of the Al_2O_3–ZrO_2–Er_2O_3 system

S.M. Lakiza *, L.M. Lopato

Frantsevich Institute for Problems of Materials Science, Krzizanovsky 3, 03142 Kyiv, Ukraine

Available online 6 March 2008

Abstract

The phase diagram of the Al_2O_3–ZrO_2–Er_2O_3 system was constructed in the temperature range 1200–2800 °C. The phase transformations in the system are completed in eutectic reactions. No ternary compounds or regions of substantial solid solution were found in the components or binaries in this system. Four ternary and three binary eutectics were found first. The minimum melting temperature is 1720 °C and it corresponds to the ternary eutectic Al_2O_3 + F-ZrO_2 + $Er_3Al_5O_{12}$. The solidus surface projection, the schematic of the alloy crystallization path and the vertical sections present the complete phase diagram of the Al_2O_3–ZrO_2–Er_2O_3 system.

Keywords: Phase diagram; Al_2O_3; ZrO_2; Er_2O_3

1. Introduction

The investigation of the Al_2O_3–ZrO_2–Er_2O_3 phase diagram is the part of systematic investigation of ternary phase diagrams including alumina, zirconia and oxides of lanthanides. Erbia is an effective ZrO_2 stabilizer.[1] Alumina improves thermo mechanical properties of zirconia ceramics and its hydrothermal stability.[2–4] The Al_2O_3–ZrO_2–Er_2O_3 system contains new ternary and binary eutectics which are perspective to obtain structural high-temperature oxide ceramic materials by directional solidification.[5]

The phase diagrams of the bounding binary systems have been examined in some detail.[6–19] The Al_2O_3–ZrO_2 system is of the eutectic type and is described elsewhere.[6] The Al_2O_3–Er_2O_3 system[7–12] includes three compounds: congruently melting at 1960 °C $Er_3Al_5O_{12}$ (Er_3A_5) with garnet-like structure, congruently melting at 1963 °C $ErAlO_3$ (ErA) with perovskite-like structure and congruently melting at 1990 °C $Er_4Al_2O_9$ (Er_2A) with monoclinic structure. No substantial solubility regions on the base of the components and binary compounds were found in the Al_2O_3–Er_2O_3 system. The phase transformations of Er_2O_3 X ⇆ H ⇆ A ⇆ B ⇆ C (X, H, A, B, C—phases on the base of Er_2O_3 with high-temperature cubic (X), high-temperature hexagonal (H), low-temperature hexagonal (A), monoclinic (B) and low-temperature cubic (C) structures of rare-earths oxides) realize as H ⇆ C transformation in the very narrow temperature interval about 2320 °C,[12] while X ⇆ H transformation realizes very close to the Er_2O_3 melting temperature (2390 °C). Therefore, we take the H ⇆ C phase transformation as united one. It displays on the liquidus surface as metatectic point with 2320 °C, 96 mol% Er_2O_3 coordinates. Four eutectics were detected in the system: Al_2O_3(AL) + Er_3A_5 at 1810 °C, 19 mol% Er_2O_3, Er_3A_5 + ErA at 1930 °C, 42.5 mol% Er_2O_3, ErA + Er_2A at 1920 °C, 57 mol% Er_2O_3 and Er_2A + C at 1880 °C, 74 mol% Er_2O_3.

The system ZrO_2–Er_2O_3 investigated in the 1250–2700 °C range is one of the eutectic type with eutectic coordinates 2350 °C, 82 mol% Er_2O_3.[13–19] A peritectic point L + F ⇆ C with coordinates 2400 °C, 75 mol% Er_2O_3 was found on the liquidus curve. Wide ranges of solid solutions with fluorite-like F, tetragonal T and monoclinic structures M on the base of ZrO_2 with different Er_2O_3 content were found in the system. Wide range of solid solutions with cubic structure C-Er_2O_3 was found on the base of Er_2O_3. A compound-superstructure $Er_4Zr_3O_{12}$ (Er_2Z_3)[15] with a rhombohedral-type structure was found in the F solid-solution field below 1490 °C having no homogeneity area.[15,16] The phase transformations of ZrO_2 F ⇆ T ⇆ M and Er_2O_3 (H ⇆ C) take place in the solid state and are not seen on the liquidus curves. The nature of these transformations is eutectoid.

Systematic information about the interaction in the system Al_2O_3–ZrO_2–Er_2O_3 is absent in the literature. In a computer simulation the Al_2O_3–ZrO_2–Er_2O_3 liquidus surface

* Corresponding author. Tel.: +380 44 424 35 73; fax: +380 44 424 21 31.
E-mail address: sergij_lakiza@ukr.net (S.M. Lakiza).

0955-2219/$ – see front matter © 2008 Elsevier Ltd. All rights reserved.
doi:10.1016/j.jeurceramsoc.2008.01.012

using a CALPHAD method based on experimental results on bounding binaries was done.[5] Single alloys in Al_2O_3-rich area of the ternary system were investigated to specify the composition of Al_2O_3-rich ternary eutectic. The composition without primary crystals was determined with mole ratio of $Al_2O_3/Er_2O_3/ZrO_2 = 65.9/15.5/18.6$.

In this investigation the Al_2O_3–ZrO_2–Er_2O_3 phase diagram is presented as isothermal sections at 1250 and 1650 °C, liquidus and solidus projections on the concentration triangle, phase diagrams of the triangulating sections, schematic of the reactions proceeding during equilibrium crystallization of melted samples and three isopleths in a wide range of temperatures and concentrations. The temperatures of isothermal sections were chosen according to the temperature stability interval for the superstructures $Ln_2Zr_2O_7$ and $Ln_4Zr_3O_{12}$ in the bounding binary systems ZrO_2–Ln_2O_3, where Ln = lanthanides. The upper temperature stability limits for these superstructures depending on the atomic lanthanides numbers are presented in a previous work.[20]

The analysis of interaction in the binaries Al_2O_3–Y_2O_3 and Al_2O_3–Er_2O_3 showed the similarity,[6,10] which is given by the closeness of Er (0.881) and Y (0.892) ionic radii.[21] It allowed to assume that the interaction in the system Al_2O_3–ZrO_2–Er_2O_3 should be similar to the interaction in the system Al_2O_3–ZrO_2–Y_2O_3 and determined by the structure of bounding systems in the absence of ternary compounds and appreciable solubility areas. In this case the interaction in the ternary system consists in equilibria of binary compounds Er_3A_5, ErA and Er_2A from the bounding system Al_2O_3–Er_2O_3 with solid solutions F and Er_2Z_3 phase from the bounding system ZrO_2–Er_2O_3 as well as component oxides and phases on their base. Triangulation of the system will be realized using Er_3A_5–F, ErA–F and Er_2A–F sections.

2. Experimental details

Specimens were obtained by both chemical method and from melting the component oxides. Powders of alumina (99.9%), zirconia (99.99%), erbia (99.9%) from Donetskij zavod khimreaktiviv, Donetsk, were used as raw materials. The appropriate quantities of oxides were blended in an agate mortar with ethanol, dried and pressed into pellets 5 mm in diameter and 5 mm in height.

Powders of $Al(NO_3)_3{\cdot}9H_2O$, $ZrO(NO_3)_2{\cdot}2H_2O$ with purity 99.9% (Donetskij zavod khimreaktiviv, Donetsk) and erbia (99.9%) were used for chemical route preparations. Both salts and erbia were dissolved in water with some droplets of concentrated nitric acid added, dried, calcined at 900 °C in air and pressed into pellets of the same dimensions. The specimens were taken at 5–10 mol% intervals on the bisector with an Al_2O_3/ZrO_2 ratio of 1, an isopleth 20 mol% ZrO_2 and along the section ErA–ZrO_2. Compositions of experimental samples are seen in the corresponding pictures. Additional compositions were chosen in the process of identifying the location of the ternary eutectic points. For the constructing of isothermal sections chemically derived samples were annealed at 1250 and 1650 °C for the time necessary to attain equilibrium, established by unchanging XRD patterns. Other samples were fired

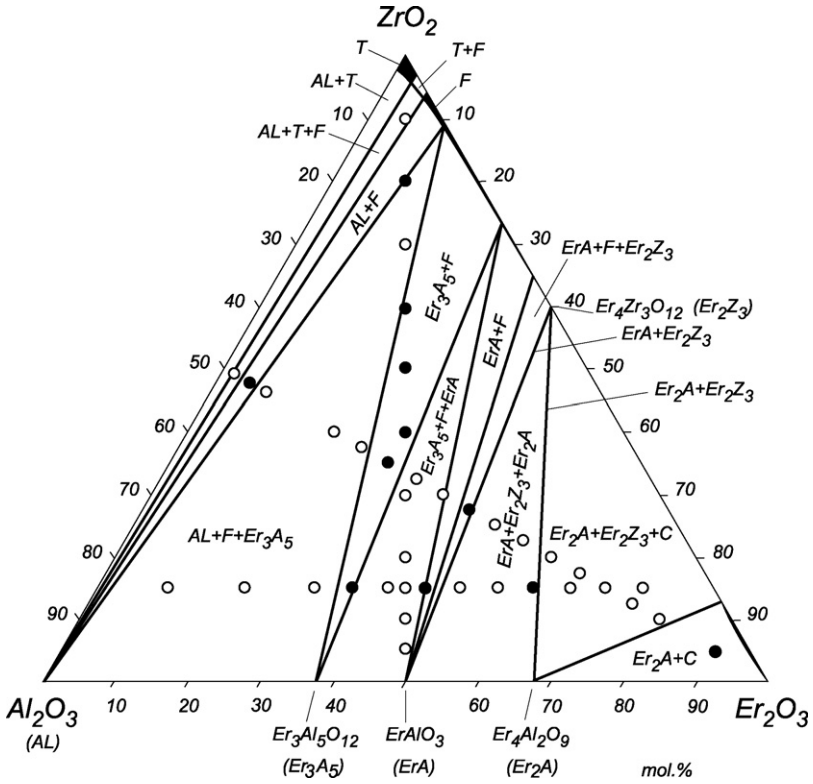

Fig. 1. Isothermal section of the Al_2O_3–ZrO_2–Er_2O_3 phase diagram at 1250 °C: (●) two-phase samples; (○) three-phase samples.

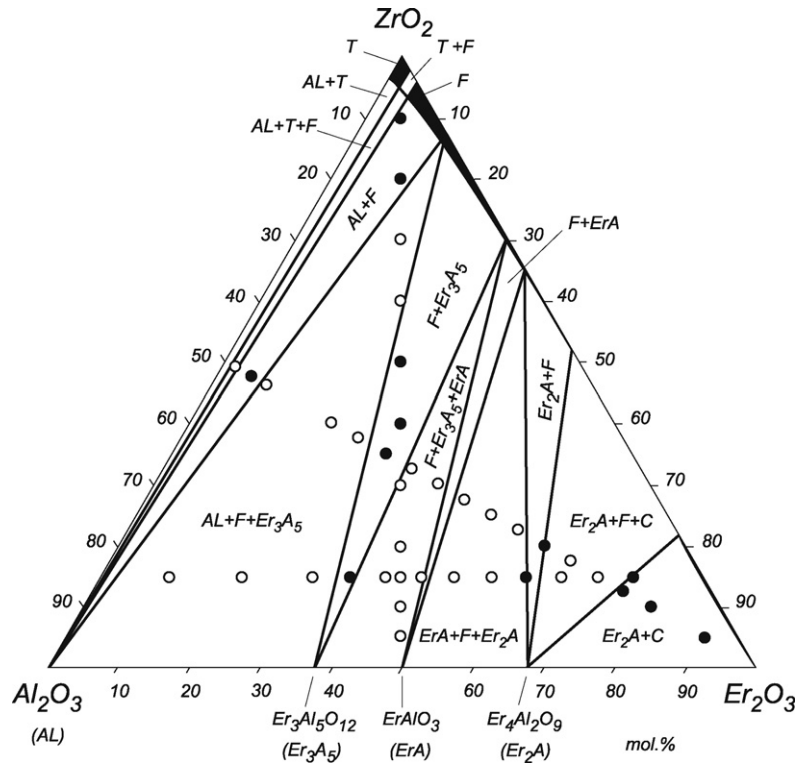

Fig. 2. Isothermal section of the Al_2O_3–ZrO_2–Er_2O_3 phase diagram at 1650 °C: (●) two-phase samples; (○) three-phase samples.

at 1250 °C in air for 6 h then melted in molybdenum pots in a DTA device[22] at total pressure of H_2 about 1.2 atm and annealed below the solidus temperature for 1 h. The specimens were investigated by DTA in H_2 at temperatures to 2300 °C, X-ray (DRON-1.5, Burevestnik, St.-Petersburg), petrographic (MIN-8 optical microscope, LOMO, St.-Petersburg) and microstructure phase (ZEISS DSM982 GEMINI) analysis. The accuracy for XRD measurement came to ±0.0003 nm, for refractive indexes measured with immerse liquids ±0.003, with alloys ±0.02.

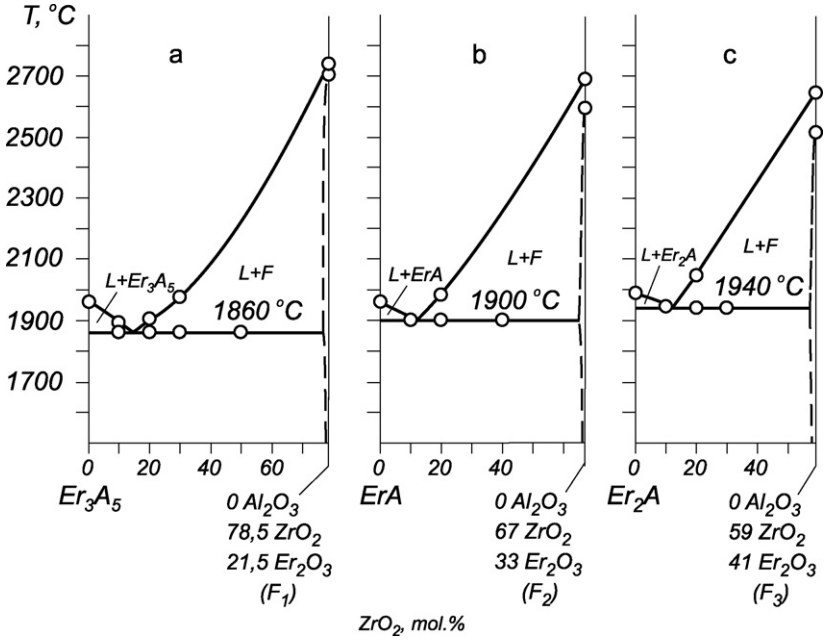

Fig. 3. Partially quasibinary sections of the Al_2O_3–ZrO_2–Er_2O_3 phase diagram: (a) Er_3A_5–F_1; (b) ErA–F_2; (c) Er_2A–F_3.

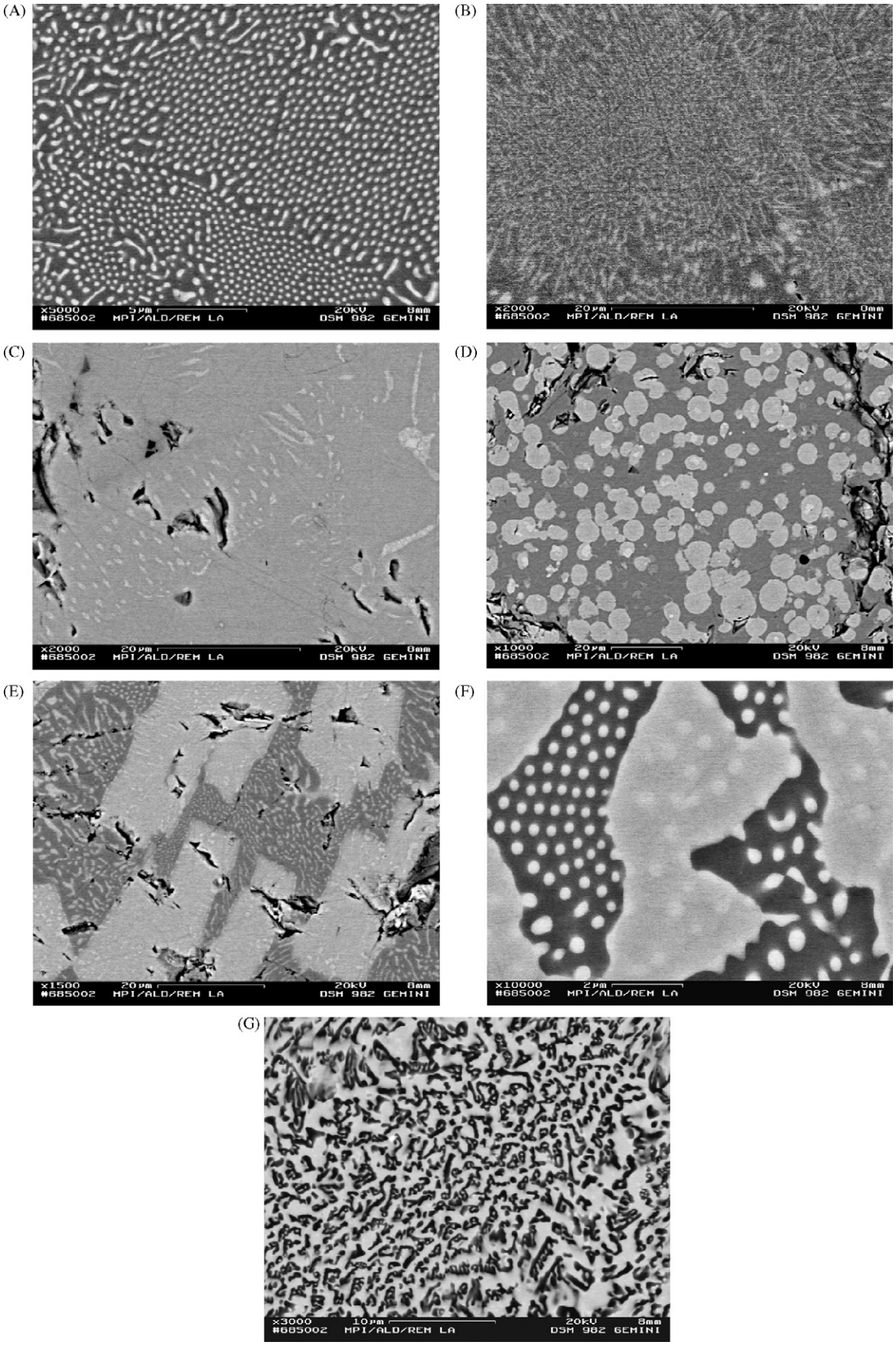
(A)
x5000 5μm 20kV 8mm
#685002 MPI/ALD/REM LA DSM 982 GEMINI
(B)
x2000 20μm 20kV 8mm
#685002 MPI/ALD/REM LA DSM 982 GEMINI
(C)
x2000 20μm 20kV 8mm
#685002 MPI/ALD/REM LA DSM 982 GEMINI
(D)
x1000 20μm 20kV 8mm
#685002 MPI/ALD/REM LA DSM 982 GEMINI
(E)
x1500 20μm 20kV 8mm
#685002 MPI/ALD/REM LA DSM 982 GEMINI
(F)
x10000 2μm 20kV 8mm
#685002 MPI/ALD/REM LA DSM 982 GEMINI
(G)
x3000 10μm 20kV 8mm
#685002 MPI/ALD/REM LA DSM 982 GEMINI

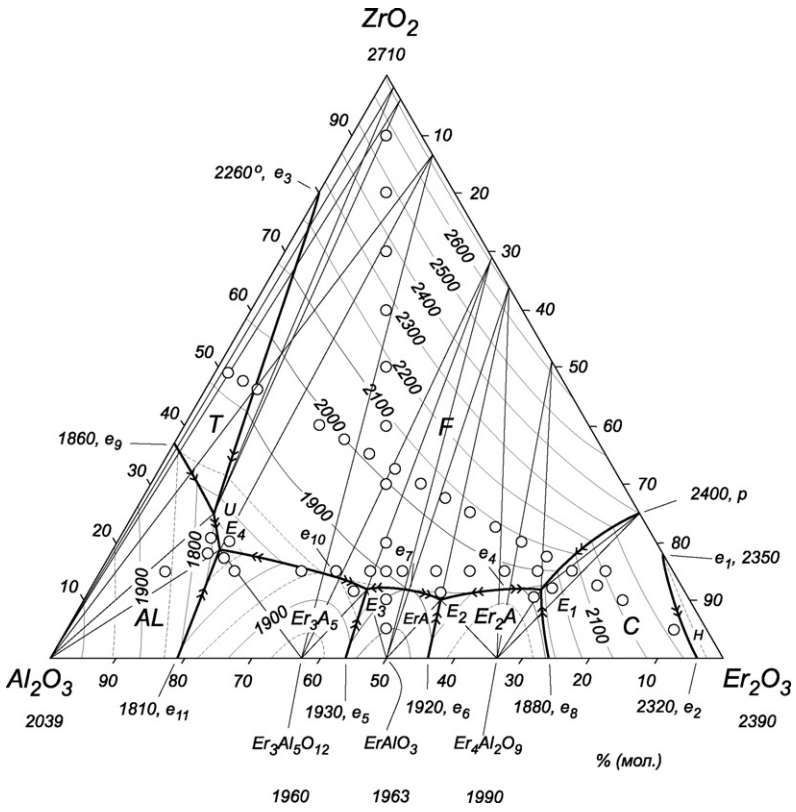

Fig. 5. Projection of the liquidus surface for the Al_2O_3–ZrO_2–Er_2O_3 phase diagram.

As far as wide areas of solid solutions F exist in the binary bounding system ZrO_2–Er_2O_3, so we used the compositional dependence of lattice parameter a_F to determine conoid triangles coordinates in the system.[15]

3. Results and discussion

Two isothermal sections at 1250 and 1650 °C were constructed incorporating literature data and the XRD results obtained (Figs. 1 and 2). No ternary compounds or regions of extraordinary solid solutions were found in the components or binaries except small regions of ternary solid solutions in the ZrO_2 corner. They appeared because of limited Al_2O_3 and Er_2O_3 solubility in ZrO_2 at elevated temperatures. Both isothermal sections are similar and differ only in the width of phase fields and that at 1250 °C the phase ErA equilibrates not only with F solid solution, as at 1650 °C, but also with the phase Er_2Z_3, which is stable below 1490 °C. Thus new ternary regions ErA + F + Er_2Z_3 and ErA + Er_2Z_3 + Er_2A as well as new narrow binary regions ErA + Er_2Z_3 and Er_2Z_3 + Er_2A appear in the section at 1250 °C.

The existence of two-phase regions AL + F, Er_3A_5 + F, ErA + F and Er_2A + F makes it possible to accept them as triangulating sections of the system Al_2O_3–ZrO_2–Er_2O_3. As far as phase F is of a variable composition then these sections can be estimated as partially quasibinary. So as to verification of this hypothesis we constructed vertical sections Er_3A_5–F_1, ErA–F_2 and Er_2A–F_3 of the Al_2O_3–ZrO_2–Er_2O_3 phase diagram. The specimens were taken at 5 mol% intervals in the middle of two-phase fields, established in the isothermal section of the phase diagram at 1650 °C.

Phase diagrams of the partially quasibinary sections of the Al_2O_3–ZrO_2–Er_2O_3 phase diagram are presented in Fig. 3 in the 1500–1700 °C interval. The sections are of the eutectic type and exhibit no remarkable solid solubility. The coordinates of the eutectic points are 14 mol% ZrO_2, 1860 °C (Er_3A_5 + F_1 (21.5 mol% Er_2O_3)), 12 mol% ZrO_2, 1900 °C (ErA + F_2 (33 mol% Er_2O_3)) and 12 mol% ZrO_2, 1940 °C (Er_2A + F_3 (41 mol% Er_2O_3)). Their microstructures are presented in Fig. 4A–C. At the same time these quasibinary eutectic points are saddle points in the phase diagram of the Al_2O_3–ZrO_2–Er_2O_3 system.

The liquidus surface for the Al_2O_3–ZrO_2–Er_2O_3 phase diagram in conjunction with conoid triangles (Alkemade lines) is shown in Fig. 5. It consists of eight fields for primary crystalliza-

Fig. 4. Microstructures of some alloys in the Al_2O_3–ZrO_2–Er_2O_3 system, mol%. (A) Saddle point 51Al_2O_3–14ZrO_2–35Er_2O_3 (e_{10}): dark phase, Er_3A_5; light phase, F_1; (B) saddle point 40Al_2O_3–12ZrO_2–48Er_2O_3 (e_7): dark phase, ErA; light phase, F_2; (C) saddle point 26Al_2O_3–12ZrO_2–62Er_2O_3 (e_4): dark phase, Er_2A; light phase, F_3; (D) ternary eutectic point 21Al_2O_3–12ZrO_2–67Er_2O_3 (E_1): dark matrix phase, Er_2A; large isotropic light phase, C-Er_2O_3; little isotropic light phase, F; (E) ternary eutectic point 37Al_2O_3–10ZrO_2–53Er_2O_3 (E_2): dark matrix phase, ErA; large rectangular light phase, Er_2A; light inclusions in ErA and Er_2A phases, F; (F) ternary eutectic point 47Al_2O_3–12ZrO_2–41Er_2O_3 (E_3): dark phase, Er_3A_5; grey phase, ErA; light inclusions in Er_3A_5 and ErA phases, F; (G) ternary eutectic point 65Al_2O_3–19ZrO_2–16Er_2O_3 (E_4): dark phase, Al_2O_3; light phase, Er_3A_5; light inclusions in Al_2O_3 phase, F.

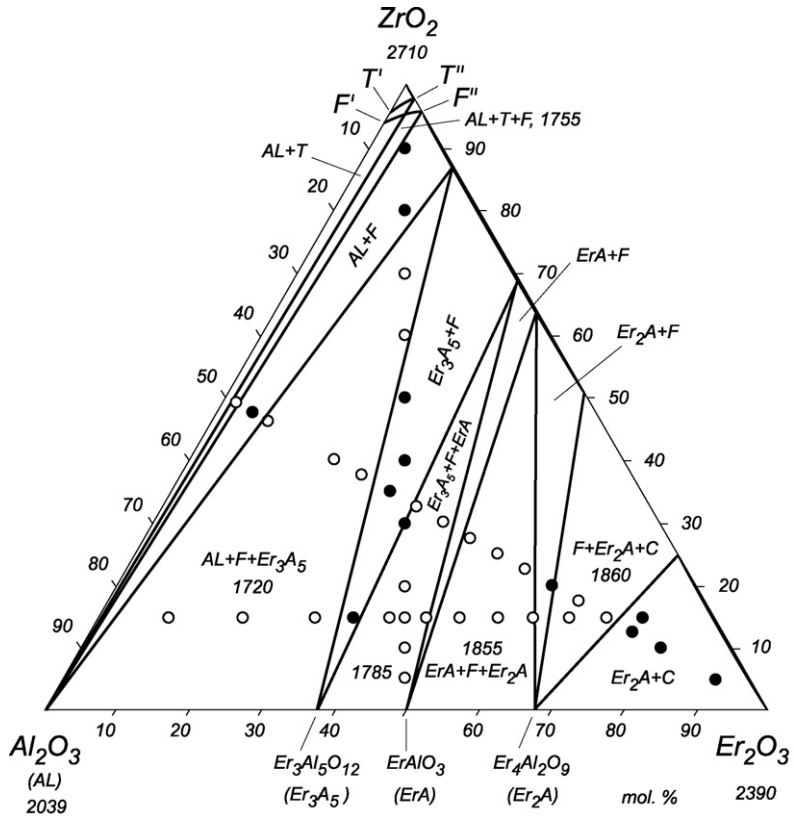

Fig. 6. Solidus surface projection for the Al_2O_3–ZrO_2–Er_2O_3 phase diagram: (●) two-phase samples; (◯) three-phase samples.

tion. Every component and binary compound has its own field. No new phases or regions of remarkable solid solution were found in the components or binaries in the Al_2O_3–ZrO_2–Er_2O_3 system. The largest liquidus area is occupied by solid solutions of Er_2O_3 in ZrO_2. This field is divided by the monovariant line ($F \leftrightarrows T + L$) into two primary crystallization fields for solid solutions with fluorite-like cubic (F) and tetragonal (T) structures. The monoclinic form of ZrO_2 has no primary crystallization field on the liquidus because it exists at temperatures that do not exceed temperatures of binary and ternary eutectics. The ZrO_2 solid solutions in Er_2O_3 with H- and C-structures of rare earth oxides have their own fields for primary crystallization. The coordinates of invariant points of the Al_2O_3–ZrO_2–Er_2O_3 phase diagram are listed in Table 1. It should be emphasized a very good agreement between the composition of E_4 obtained in this investigation and the results of Ref. 5. The microstructures of the invariant points E_1–E_4 are shown in Fig. 4D–G. The minimum melting temperature in the system is 1720 °C and relates to the ternary eutectic E_4. The maximum liquidus temperature is 2710 °C and refers to the melting point of pure ZrO_2.

The projection of the solidus surface of the Al_2O_3–ZrO_2–Er_2O_3 phase diagram is shown in Fig. 6. Data on the coordinates of the conoid triangles of solid phases on the solidus surface were obtained from XRD measurements and are given in Table 2. According to the liquidus construction, the solidus surface consists of five isothermal three-phase fields corresponding to four invariant equilibrium of the eutectic type and one of the transformation type. The linear surfaces representing the solidification ends of the monovariant eutectics AL + T, AL + F, Er_3A_5 + F, ErA + F, Er_2A + F and Er_2A + C

Table 1
Coordinates of invariant points in the Al_2O_3–ZrO_2–Er_2O_3 system

Equilibrium points	Temperature (°C)	Composition (mol%)			Invariant equilibrium
		Al_2O_3	ZrO_2	Er_2O_3	
e_4	1940	26	12	62	$L \Leftrightarrow Er_2A + F$
e_7	1900	40	12	48	$L \Leftrightarrow ErA + F$
E_1	1860	21	12	67	$L \Leftrightarrow Er_2A + F + C$
e_{10}	1860	51	14	35	$L \Leftrightarrow Er_3A_5 + F$
E_2	1855	37	10	53	$L \Leftrightarrow ErA + F + Er_2A$
E_3	1785	47	12	41	$L \Leftrightarrow Er_3A_5 + F + ErA$
U	1755	63	25	12	$L + T \Leftrightarrow F + AL$
E_4	1720	65	19	16	$L \Leftrightarrow AL + F + Er_3A_5$

Table 2
Coordinates of the apexes of the solid-phase tie-line triangles on the solidus surface of the Al_2O_3–ZrO_2–Er_2O_3 phase diagram

Phase	Composition of the equilibrium phases (mol%)						
	AL	T	F	Er_3A_5	ErA	Er_2A	C
AL + T + F	100	97.5ZrO_2–2.5Er_2O_3	96ZrO_2–4Er_2O_3	–	–	–	–
AL + F + Er_3A_5	100	–	87.5ZrO_2–12.5Er_2O_3	100	–	–	–
Er_3A_5 + F + ErA	–	–	69.5ZrO_2–30.5Er_2O_3	100	100	–	–
ErA + F + Er_2A	–	–	65ZrO_2–35Er_2O_3	–	100	100	–
Er_2A + F + C	–	–	51ZrO_2–49Er_2O_3	–	–	100	25ZrO_2–75Er_2O_3

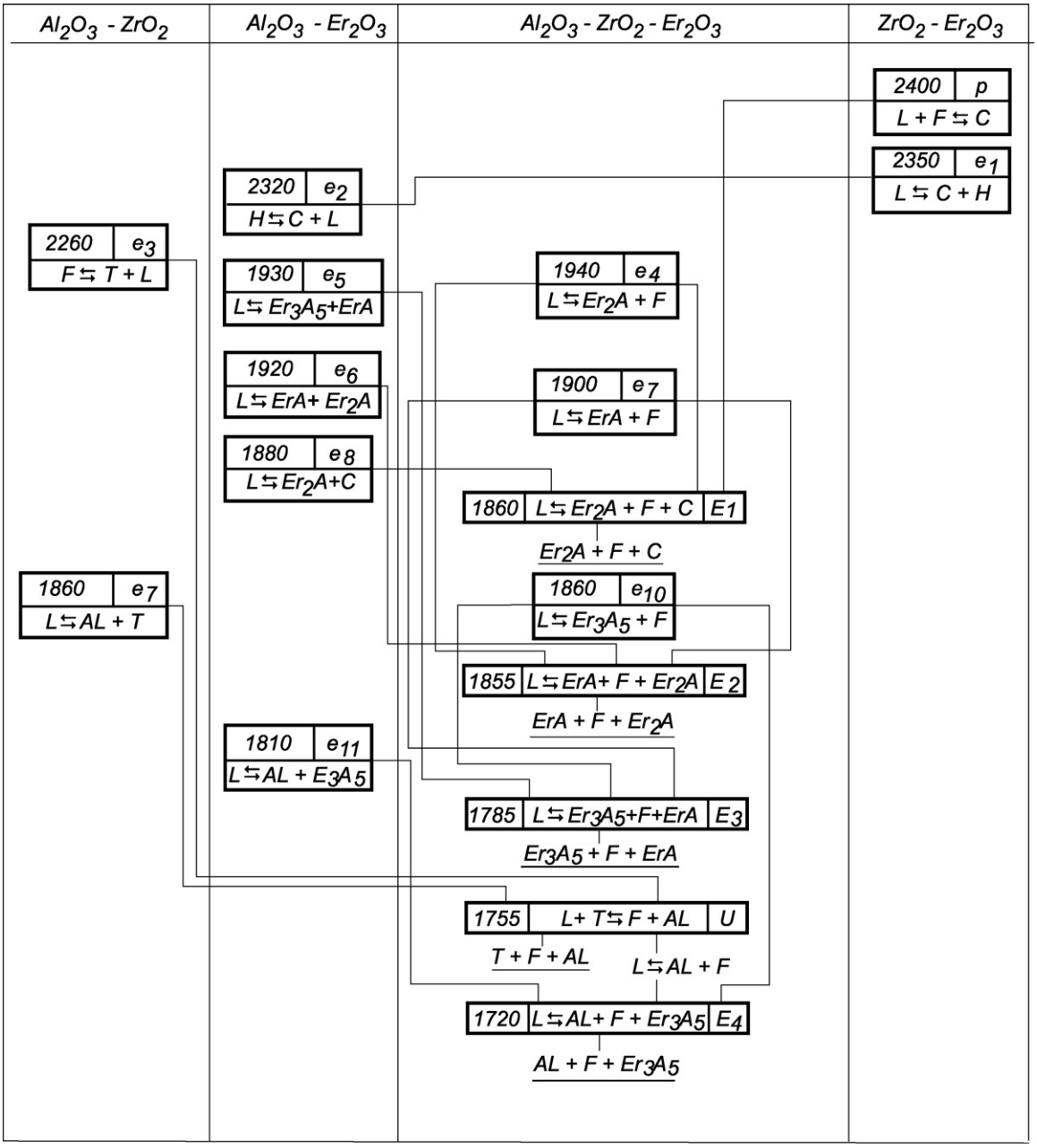

Fig. 7. Schematic of the reactions proceeding during sample crystallization in the Al_2O_3–ZrO_2–Er_2O_3 system.

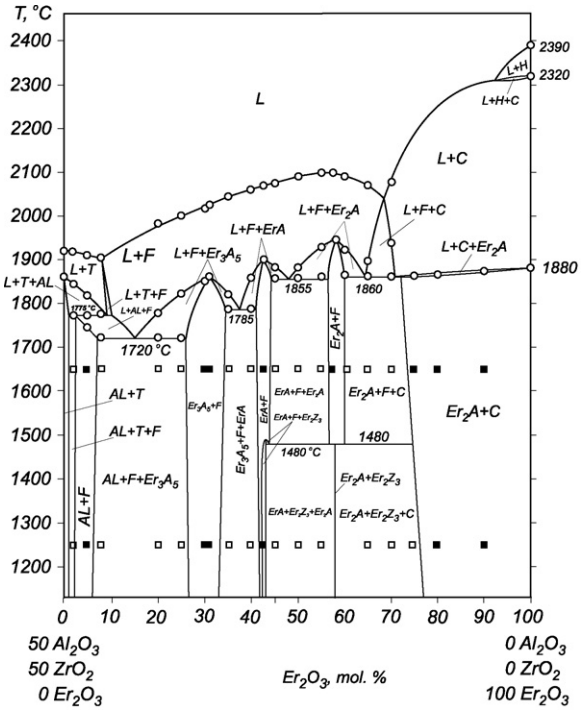

Fig. 8. Bisector $Al_2O_3/ZrO_2 = 1$ for the Al_2O_3–ZrO_2–Er_2O_3 phase diagram.

are the parts of the solidus too. Two linear surfaces are also the solidus part: for the F solid solutions crystallization end, that is adjacent to the boundary system ZrO_2–Er_2O_3 in the 4–49 mol% Er_2O_3 interval, and the linear surface $F'T'F''T''$ formed by the end of conoid triangles, which rest upon the

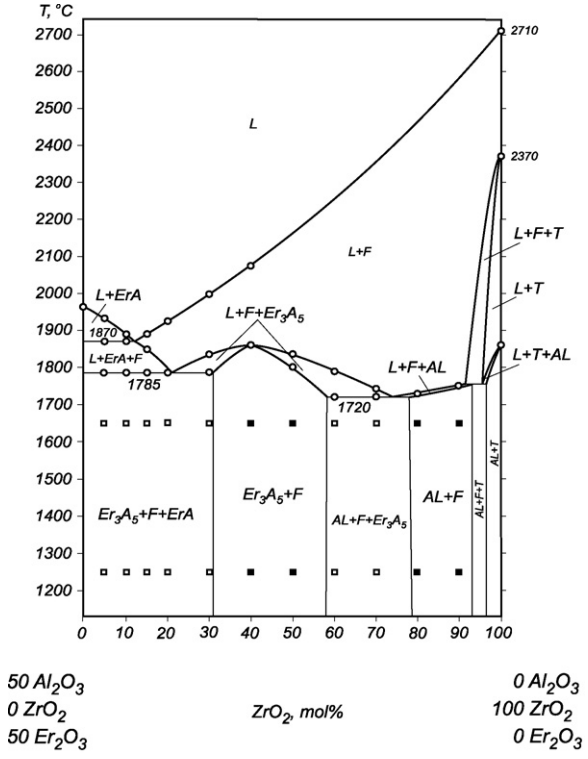

Fig. 9. Bisector $Al_2O_3/Er_2O_3 = 1$ for the Al_2O_3–ZrO_2–Er_2O_3 phase diagram.

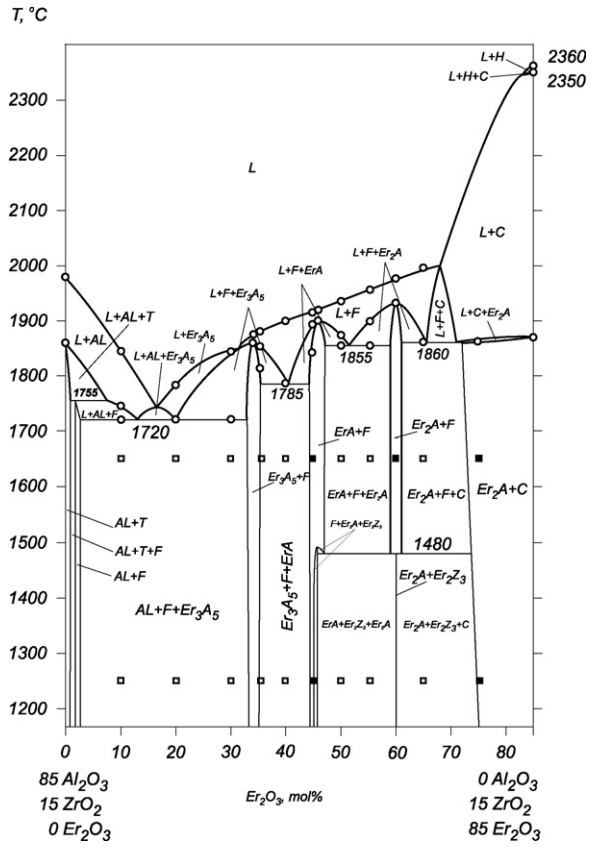

Fig. 10. Isopleth 15 mol% ZrO_2 for the Al_2O_3–ZrO_2–Er_2O_3 phase diagram.

equilibrium phases T and F whose compositions are located near the ZrO_2 apex and move upon curves $T'T''$ and $F'F''$. The isothermal field AL + T + F that corresponds to invariant transformation equilibrium $L + T \leftrightarrows F + AL$ (U, 1755 °C) is the part of quadrant, where the transformation reaction finishes with total liquid expenditure.

On the base of data on liquidus, solidus and bounding binary systems, a schematic of the reactions that proceed during the equilibrium crystallization of the Al_2O_3–ZrO_2–Er_2O_3 system alloys is shown in Fig. 7. The equilibrium crystallization in this system is characterized with one invariant four-phase transformation process at 1755 °C (U), four invariant four-phase congruent processes at 1850 (E_1), 1855 (E_2), 1785 (E_3) and 1720 °C (E_4) and three invariant three-phase congruent processes at 1940 (e_4), 1900 (e_7) and 1860 °C (e_{10}) (Fig. 7).

Three polythermal sections were constructed to present the phase diagram of the Al_2O_3–ZrO_2–Er_2O_3 system more completely: bisectors $Al_2O_3/ZrO_2 = 1$, $Al_2O_3/Er_2O_3 = 1$ and isopleth 15 mol% ZrO_2 (Figs. 8–10). These figures confirm the triangulation and discover the interaction in different parts of the Al_2O_3–ZrO_2–Er_2O_3 phase diagram.

4. Conclusions

The phase diagram of the Al_2O_3–ZrO_2–Er_2O_3 system was constructed in the temperature range 1250–2800 °C. The liquidus surface of the phase diagram reflects the preferentially eutectic interaction in the system. Four ternary and three binary

eutectics were found. No ternary compounds or regions of remarkable solid solution were found in the components or binaries in this ternary system. The minimum melting temperature is 1720 °C and it corresponds to the ternary eutectic Al_2O_3 + F-ZrO_2 + $Er_3Al_5O_{12}$. The polythermal sections present the complete phase diagram of the Al_2O_3–ZrO_2–Er_2O_3 system.

References

1. Stewart, R. K. and Hunter Jr., O., Stabilization of zirconia by erbia. *J. Am. Ceram. Soc.*, 1970, **53**(7), 421–422.
2. Sakka, Y., Suzuki, T. S., Morita, K. and Hiraga, K., Colloidal processing and superplastic properties of fine-grained zirconia-based ceramics. *Key Eng. Mater.*, 2002, **206–213**, 645–648.
3. Gregorova, E., Havrda, J. and Pabst, W., ATZ ceramics prepared by slip-casting and centrifugal slip casting. *Key Eng. Mater.*, 2002, **206–213**, 369–372.
4. Rodriquez-Pulido, A., Ross, I. M. and Rainforth, W. M., Processing and structural characterization of 3Y-TZP ceramics resistant to hydrothermal ageing. *Key Eng. Mater.*, 2002, **206–213**, 1053–1056.
5. Waku, Y., Sakata, S., Mitani, A., Shimizu, K., Ohtsuka, A. and Hasebe, M., Microstructure and high-temperature strength of Al_2O_3/$Er_3Al_5O_{12}$/ZrO_2 ternary melt growth composite. *J. Mater. Sci.*, 2005, **40**, 711–717.
6. Lakiza, S. M. and Lopato, L. M., Stable and metastable phase relations in the system alumina–zirconia–yttria. *J. Amer. Ceram. Soc.*, 1997, **80**(4), 893–902.
7. Bertaut, F. and Forrat, F., Etude des combinaisons des oxydes des terres rares avec l'alumine et la galline. *C. R. Acad. Sci., Paris*, 1956, **243**(17), 1219–1222.
8. Schneider, S. J., Roth, R. S. and Waring, J. L., Solid state reactions involving oxides of trivalent cations. *J. Res. Nat. Bur. Stand.*, 1961, **65A**(4), 345–374.
9. Mizuno, M., Yamada, T. and Nogushi, T., Phase diagrams of the systems Al_2O_3–Ho_2O_3 and Al_2O_3–Er_2O_3 at high temperatures. *J. Ceram. Soc. Jpn.*, 1979, **87**(8), 404–412.
10. Wu, P. and Pelton, A. D., Coupled thermodynamic-phase diagram assessment of the rare earth oxide-aluminum oxide binary systems. *J. Alloys Compd.*, 1992, **179**, 259–287.
11. Yamane, H., Ogawara, K., Omori, M. and Hirai, T., Phase transition of rare-earth aluminates ($RE_4Al_2O_9$) and rare earth gallates. *J. Am. Ceram. Soc.*, 1995, **78**(9), 2385–2390.
12. Lopato, L. M., Shevchenko, A. V., Kuschevskij, A. E. and Tresvjatskij, S. G., Polymorph transformation of rare-earth elements oxides at high temperatures. *Izv. AN SSSR. Neorgan. Mater.*, 1974, **10**(8), 1481–1487.
13. Thornber, M. R., Bevan, D. J. M. and Summerville, E., Mixed oxide of the type MO_2 (fluorite)–M_2O_3. V. Phase studies in the system ZrO_2–M_2O_3 (M–Sc, Yb, Er, Dy). *J. Solid State Chem.*, 1970, **1**(3/4), 545–553.
14. Rouanet, A., Contribution a l'etude des systemes zircone-oxydes des lanthanides au voisinage de la fusion. *Rev. Int. Hautes Temp. Refract.*, 1977, **8**(2), 161–180.
15. Duran, P., The system erbia–zirconia. *J. Am. Ceram. Soc.*, 1977, **60**(11–12), 510–513.
16. Pascual, C. and Duran, P., Phase equilibria and ordering in the erbia–zirconia system. *J. Mater. Sci.*, 1981, **16**(11), 3067–3076.
17. Lopato, L. M., Red'ko, V. P., Gerasimjuk, G. I. and Shevchenko, A. V., Synthesis of some zirconates (hafnates) REE, *Poroshkovaja Metall.*, 1990, (4), 73–75.
18. Yoshima, M., Noma, T., Ishizava, N. and Yoshimura, M., Stable and metastable phase relationships in the system ZrO_2–$ErO_{1.5}$. *J. Am. Ceram. Soc.*, 1991, **74**(3), 510–513.
19. Andrijevskaja, E. R., Lopato, L. M. and Shevchenko, A. V., Liquidus surface for the system ZrO_2–Y_2O_3–Er_2O_3. *Neorgan. Mater.*, 1996, **32**(6), 721–726.
20. Lakiza, S. M. and Lopato, L. M., Phase diagram of the Al_2O_3–ZrO_2–Nd_2O_3. *J. Eur. Ceram. Soc.*, 2006, **26**, 3725–3732.
21. Shannon, R. D. and Prewitt, C. T., Effective ionic radii in oxides and fluorides. *Acta Cryst.*, 1969, **B25**(5), 924–946.
22. Lopato, L. M., Shevchenko, A. V. and Kuschevskij, A. E., Investigation of the refractory oxides system, *Poroshkovaja Metall.*, 1972, (1), 88–92.